Color Phenomenon in Post-Transition-Metal Salts[†]

S. P. MCGLYNN,* T. AZUMI, and D. KUMAR

Physikalisches Institut, Universität Bonn, 5300 Bonn 1, Federal Republic of Germany, Choppin Chemical Laboratories, Louisiana State University, Baton Rouge, Louisiana 70803, and Department of Chemistry, Tohoku University, Sendai 980, Japan

Contents

Tohru Azumi received his undergraduate and graduate training in the Department of Chemistry, Faculty of Science, Tohoku University, Sendai, Japan. During the years 1961–1964 he studied as a Fulbright graduate student in the Department of Chemistry, Louisiana State University, Baton Rouge, LA, under Professor S. P. McGlynn. In 1966 he joined the research group of Professors S. Nagakura and M. Ito of the Institute for Solid State Physics, University of Tokyo. He has been a faculty member in the Department of Chemistry, Faculty of Science, Tohoku University, since 1969.

Sean P. McGlynn received his B.Sc. (Honors) and M.Sc. at University College Galway, Galway, Ireland, in 1951 and 1952, respectively. He obtained his Ph.D. from Florida State University in 1956 in molecular electronic structure under Professor Michael Kasha. He studied as a postdoctoral fellow with Professor W. Simpson at the University of Washington (Seattle) during 1956–1957. Since then, apart from a brief stint on the Biophysics Faculty at Yale University, he has been employed at The Louisiana State University, where he is now Boyd Professor. He has published two books and over 200 articles. He has received many awards, among them The Florida Award of the American Chemical Society (1970), The Southwest Regional Award of the American Chemical Society (1967), and the Senior U.S. Scientist Award of the von Humboldt Foundation.

Devendra Kumar was born and educated in Delhi, India. He obtained B.Sc., M.Sc., and Ph.D. degrees in physics from Delhi University. He started teaching at K. M. College, Delhi, after getting the M.Sc. degree in 1965. His Ph.D. work was in the field of microwave spectroscopy. Presently, he is a postdoctoral research associate at Louisiana State University (on leave from Delhi University). His current research interests are in photoacoustic spectroscopy using lasers.

TABLE I: Colors of Nitrite and Chlorite Salts

cation M	nitrite anion,[a] NO_2^-		chlorite anion,[c] ClO_2^-	
	ϵ[b]	color	color	comment
NH_4(I)	3×10^{-3}	none	none	crystal
Na(I)	3×10^{-3}	none	none	crystal
K(I)	3×10^{-3}	none	none	crystal
Ba(II)		yellowish	none	crystal
Cd(II)	2.3×10^{-2}	yellowish	yellow	solution
Ag(I)	0.5	yellow	green yellow	crystal[d]
Pb(II)	11.7	orange yellow	orange yellow	crystal
Tl(I)	0.64	orange	yellow	solution
Hg(I)		sulfur yellow	red	crystal[e]

[a] From H. J. Maria, A. Wahlborg, and S. P. McGlynn, *J. Chem. Phys.*, **48**, 4694 (1968). [b] The molar decadic extinction coefficient, ϵ, for NH_4(I), Na(I), and K(I) is based on *total* nitrite present. That for the remaining salts is based on total concentration of $M_x(NO_2)$, where x is not necessarily an integer. For details, see footnote a. [c] Observations by H. J. Maria and S. P. McGlynn, unpublished. [d] Crystal structure of $AgClO_2$ is unsettled. One set of authors [R. Curti, V. Riganti, and S. Rocchi, *Acta Crystallogr.*, **10**, 687 (1957)] find it planar and covalent [i.e., r(Ag-Cl) = 2.20 Å]. Another set [J. Cooper and R. E. Marsh, *ibid.*, **14**, 202 (1961)] find it to be a distorted triangular prism structure with no direct Ag-Cl bond and, hence, electrovalent. [e] Color may be caused by $3Hg(ClO_2)_2 \cdot HgO$ impurity.

I. Introduction

This work is concerned with color phenomena in heavy-metal salts. If neither anion nor cation is separately chromophoric, the phenomenon of interest is the *induction of color* in the salt. If either the anion or cation (or both) is separately chromophoric, the phenomenon of interest is the *alteration of color* in the salt. The class of cations considered is restricted to the nontransition metals. This restriction is largely one of convenience: It evades the prolixity attendant to any discourse about intrashell (d or f) transitions, and it avoids the ambiguity associated with assignment of anionic transitions in a spectral region already crowded with intrashell excitations of the cation. Consequently, it is emphasized that the exclusion of transition-metal cations is entirely tactical and that the phenomena discussed here for non-transition-metal salts will also be found to occur in transition-metal salts.

The field of inquiry is both large and disparate. Possibly because of this, most experimental measurements are qualitative and, often, they refer to undefined chemical systems. Worse, there exists no coherent theory which can guide experiment and, as a result, the available data are "scatter-shot", disconnected, and very difficult to assimilate. The primary purpose of this work is to provide such a theory and, within the confines of that theory, to extract from the available data base those observations which are pertinent to the problem posed in the previous paragraph. It would be silly to assert tht the theoretical notions presented here are either complete or correct. However, we do assert that they provide a conceptual frame within which experiments can be conceived and phrased and that, at the present level of knowledge, they enable us to construct a pertinent and valuable interface with experiment.

II. Phenomenon and Procedure

1. The Color Phenomenon

The phenomenon of interest, namely that post-transition-metal cations often induce striking colorations, is illustrated in Table I. This phenomenon has puzzled many observers. The first definitive statement is due to Bichowsky,[1] who remarked that when the color of a compound deviates from the sum of its constituent ion colors, the electrons are no longer acted on by only one nucleus but by both. This remark contains two imputations. The first, now known as *the principle of additivity of ionic colors*, has been discussed by Pitzer[2] and Jorgensen.[3] The second, the kernel of any interpretation of deviations from the above principle, implies mutual perturbation of the anion/cation centers. The effects of this perturbation are usually categorized as (a) color induction by a cation ← anion charge transfer (CT) transition,[2] (b) cationic polarization of the anion[4] with concomitant shift, usually to lower energy, of a localized excitation (LE) of the anion, or (c) a cation-induced geometric distortion of the anion,[5] with results similar to (b).

These mechanisms are surely responsible for some color alterations. However, without addition of a fourth possibility, namely, (d) an enhancement of transitions which are forbidden in the free anion,[6] the above set is inadequate. The forbidden transitions in question may be spin-forbidden triplet ← singlet (T_i ← S_0) transitions or spatially forbidden singlet ← singlet (S_i ← S_0) transitions. It is the thesis of this article that this fourth category is the dominant color-induction mechanism. However, even granted the primacy of this fourth category, the induction of allowed character into formerly forbidden anionic transitions may well require the intermediacy of higher-energy cation ← anion CT states.[7]

2. Plan of Essay

The purpose of section III is to discuss the energies of locally excited (LE) and charge-transfer (CT) states, the interaction between them (namely LE/CT interaction), and the consequences of this interaction for the energy levels of the salt. The LE states in question pertain to the individual anions, and they are discussed in sections IV with respect to each anion and the various classes of anions. The CT states, however, pertain to the whole salt. In the simplest case, namely cation ← anion CT, the CT energy is a sensitive function of metal-ion electron affinity, $A[M^+]$, and anion ionization potential, $I[A^-]$. Consequently, in an effort to acquire some feeling for CT energies, we devote some time in section III to a consideration of the magnitudes of $A[M^+]$ and $I[M^-]$.
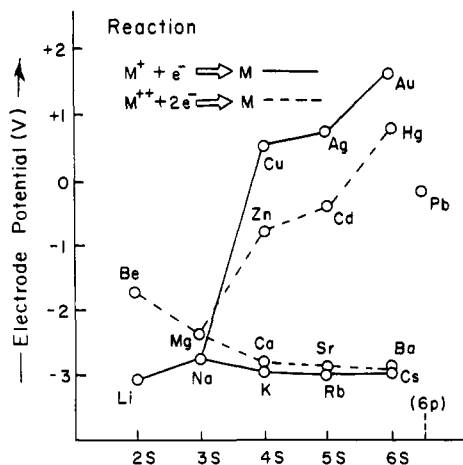
Figure 1. Electrode potentials for the reactions $M^+ + e^- \rightarrow M$ (solid line) for group 1 elements and $M^{2+} + 2e^- \rightarrow M$ (dashed line) for group 2 elements. Data are taken from the "Handbook of Chemistry and Physics", Chemical Rubber Co., Cleveland, OH, 1973. This graph may be relabelled "electron affinity" along the vertical axis (see section III.1). The data point for Pb is added for completeness.

It turns out, after imposition of LE/CT interactions, that the extremal types of electronic transitions are $^{1,3}CT \leftarrow {}^1G$ and $^{1,3}LE \leftarrow {}^1G$, where ^1G is the ground state. Since, for a given salt, it is necessary to distinguish the various transition types, we also discuss the means of experimental discrimination of $CT \leftarrow {}^1G$ and $LE \leftarrow {}^1G$ transition types on the one hand and $S_i \leftarrow {}^1G$ and $T_i \leftarrow {}^1G$ transition types on the other.

Section IV elaborates experiment and its juxtaposition to theory for various inorganic anions. This section also includes a short discussion of organic salts in order to demonstrate the distinct similarities of the organic and inorganic domains.

III. Electronic States, Transition Types, and Distinctions between Them

1. Covalency of Metal Salts

The B metals typify the post-transition metals. They have filled d orbitals and differ from the A metals (i.e., pretransition metals) in their weaker tendency to form either ions or compounds with the nonmetals. On the other hand, the B-metal ions, because of their higher electron affinities, tend to combine with polarizable anions. This tendency is evident in Figure 1, where the electrode potentials for

$$M^+ + e^- \rightarrow M \quad \text{(group 1 metals)}$$

$$M^{2+} + 2e^- \rightarrow M \quad \text{(group 2 metals)}$$
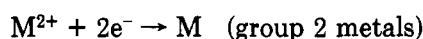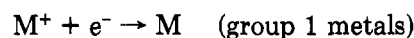
are shown. A difference of 2 to 4 V between the A and B metals is observed, and the lesser tendency of the B metals toward ionicity is obvious.

It is not surprising, then, that B-metal salts exhibit covalency. A striking example is $AgMnO_4$ which is ionic in aqueous solution and exhibits the red-purple color of MnO_4^- but which is covalent in the crystal and possesses the green color of an $AgMnO_4$ molecular unit. Further examples of this effect in Ag salts are shown[6] in Table II. It is clear from Table II, column 3, that the color of the post-transition-metal salt bears no re-

TABLE II. Colors of Silver(I) Salts

anion	color	anion $S_1 \leftarrow S_0$ absorption, nm	Ag-O r, Å	structure ref
NO_3^-	none	300	2.51	a
ClO_3^-	none	190	2.51	b
SO_4^{2-}	none	<200	2.50	c
MoO_4^{2-}	yellow	210	2.42	d
KCO_3^-	none	210	2.42	e
NO_2^-	yellow	355	2.42	f
ClO_2^-	yellow	290	2.4	g
CrO_4^{2-}	dark red		2.35	h
PO_4^{3-}	yellow	<200	2.34	i
AsO_4^{3-}	red-black	<200	2.34	c
MnO_4^-	black		2.32	j
CO_3^{2-}	yellow	210	2.30	e
SO_3^{2-}	none	<200	2.23	k

^{a} P. F. Lindley and P. Woodward, *J. Chem. Soc. A,* **123,** (1966). ^{b} I. Naray-Szabo and J. Pocza, *Z. Krist.,* **104,** 28 (1942). ^{c} L. Helmholtz and R. Levine, *J. Am. Chem. Soc.,* **64,** 354 (1942). ^{d} J. Donohue and W. Shand, *ibid.,* **69,** 222 (1947). ^{e} J. Donohue and L. Helmholtz, *ibid.,* **66;** 295 (1944). ^{f} R. E. Long and R. E. Marsh, *Acta Crystallogr.,* **15,** 448 (1962). ^{g} J. Cooper and R. E. Marsh, *ibid.,* **14,** 202 (1961). ^{h} M. L. Hackert and R. A. Jacopson, *J. Solid State Chem.,* **3,** 364 (1971). ^{i} L. Helmholtz, *J. Chem. Phys.,* **4,** 316 (1936). ^{j} E. G. Boonstra, *Acta Crystallogr., Sect. B,* **B24,** 1053 (1968). ^{k} O. Larsson, *Acta Chem. Scand.,* **23,** 2261 (1961).

lation to the lowest energy $^1LE \leftarrow {}^1G$ transition of the anion.[8] This statement also applies to certain post-transition-metal salts of MnO_4^- and CrO_4^{2-}, which do possess anionic $^1LE \leftarrow {}^1G$ transitions in the visible range but whose color is incompatible with the absorption spectrum of the isolated, free anion. It is also clear from Table II, column 4, that the degree of covalency of many silver salts is quite high [for comparison: r(Ag-O), covalent $\simeq$ 2.18 Å; r(Ag-O), ionic $\simeq$ 2.56 Å].

The degree of covalency in a given salt may be estimated from the electron affinity of the cation and the ionization potential of the anion. The former is immediately obtainable from Figure 1 for the group 1 elements. It is not, unfortunately, as readily obtainable for the group 2 elements. The electron affinity for a group 2 element refers to the process

$$M^{2+} + e^- \rightarrow M^+$$
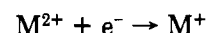
and will clearly be smaller than the redox potential. However, it appears that most of the energy change occurs during the addition of the first electron. For example, for Ca^{2+}, the addition of the first electron requires -2.50 V, whereas the addition of two electrons requires only -2.76 V. In other words, the scaling of the electrode potentials of Figure 1 as electron affinities is a good approximation even for the group 2 elements. Thus, with the addition of the extra element Pb, we can say with some confidence that the ions Ag^+, Au^+, Hg^{2+}, and Pb^{2+} possess, in a relative sense, quite high electron affinities.

2. Ionization Energies of Oxy Anions

A listing of experimental anion ionization energies $I(A^-)$ is given in Table III. Inspection of Table III indicates massive variation of the experimental numbers. For example, the SO_4^{2-} data cover a range of 5.5 eV! This variation, in part anyway, is due to the fact that the photoionization experiments refer to solid samples where contact potentials may produce a vari-

ation even within the work of the same author (e.g., 5.6 and 5.3 eV) and between different authors using essentially the same technique (e.g., 6.6 and 5.3 eV). Apart from that, it is possible that all values should be calibrated by independent means, an effort which leads, somewhat insecurely, to the value 10.8 eV for SO_4^{2-}.

In view of the above, it is difficult to place much reliability on Table III. For example, MnO_4^-, with $I[A^-]$ = 6.4 eV in Table III, is isoelectronic with MnO_3Cl, which has $I(MnO_3Cl)^9$ = 11.98 eV, and to compound the difficulty, the best available calculation[10] for MnO_4^- yields a number intermediate between these two extremes. In general, one must suspect large contact effects simply because ΔI between gaseous and (uncalibrated) solid samples is usually of the order of ~5 eV in the few cases where comparable gaseous and solid-state data exist. Consequently, any attempt to use Table III must do so with caution.

3. Configuration Interaction (CI) of Locally Excited (LE) States of Anion and Charge-Transfer (CT) States of the Anion/Cation Sytem

The whole anion/cation system will be discussed within the framework of the *composite molecule method*.[11] For simplicity, we will consider a uni-univalent system where the anion is denoted A^- and the cation is denoted M^+. Thus, the ground configuration is written $\psi(M^+, A^-) \equiv \psi_G$. The two excited configurations of interest are the LE configuration of A^-, $\psi(M^+, A^{*-})$ $\equiv \psi_{LE}$, and the CT configuration, $\psi(M, A) \equiv \psi_{CT}$. This choice of a zero-order description is convenient because we know or, at least, can estimate the zero-order energies.

In first order, we assume that CI may be confined to the two excited configurations. Thus, the ground state and the lowest-energy excited state are now written

$$\Psi_G = \psi_G$$

$$\Psi_E = a\psi_{LE} + b\psi_{CT}$$

The LE/CT mixing may cause two effects: a shift of transition energy $\Psi_E \leftarrow \Psi_G$ from the zero-order location $\psi_{LE} \leftarrow \Psi_G$ and an enhancement of the intensity of formerly weak, locally excited transitions. The intensity enhancement can be augmented further by permitting[12] ψ_{CT} and ψ_G to mix, but this need not concern us here. The energy $E(\Psi_E)$ and wave function Ψ_E (i.e., the relative magnitudes of a^2 and b^2) are sensitive to a number of factors, primary among which is the energy separation of the zero-order configurations, ψ_{LE} and ψ_{CT}.

The approximate energy of the CT configuration is $E_{CT} = I[A^-] - A[M^+] + C$ where C is the electrostatic interactions between A^- and M^+. The energy of the LE configuration may be obtained experimentally from the spectroscopy of the ionic system. Thus, the zero-order energies are at hand, and it is this fact that imbues the composite-molecule method with practicality.

Zero-order energies and those obtained from LE/CT mixing are shown in Figure 2 as a function of $I–A$. The right-hand side of the diagram corresponds to the situation $a^2 \gg b^2$ whereas the left-hand side represents the reverse. Thus, on the right-hand side $\Psi_E \simeq \psi_{LE}$, and on the left-hand side $\Psi_E \simeq \psi_{CT}$. We refer to these as the LE and CT situations, respectively. The center of

TABLE III. Ionization Energies of Oxyanions (in eV)

anion	symmetry	Source a	Source b	Source c	assorted sources
NO_2^-	C_{2v}	5.4	3.2		
ClO_2^-				3.3	
NNN^-	$D_{\infty v}$	4.8			
NO_3^-	D_{3h}	6.0	5.6		
CO_3^{2-}		5.2	5.1		
ClO_3^-	C_{3v}	5.0	11.2	5.1	
BrO_3^-			11.5		
IO_3^-			10.4		
SO_3^{2-}		6.0	9.8	4.6	
TeO_3^{2-}			10.0		
SeO_3^{2-}			9.5		
ClO_4^-	T_d	5.3	11.3	6.2	6.3^d
SO_4^{2-}		6.6	10.8	5.6	5.3^d
SeO_4^{2-}			~11.8		
PO_4^{3-}		9.0	5.2	10.5^e	
SiO_4^{4-}				5.5	
MnO_4^-				6.4	
CrO_4^{2-}				6.6	7^f
ReO_4^-					$10.0^{g,i}$
RuO_4					$12.09^{h,i}$
OsO_4					$12.32^{h,i}$

^{a} A. Calabrese and R. G. Hayes, *J. Electron Spectrosc. Relat. Phenom.*, **6**, 1 (1975). ^{b} V. I. Nefedev, Yu. A. Buslaev. N. P. Sergushin, Yu. V. Kokunov, V. V. Kovalev, and L. Bayer, *ibid.*, **6**, 221 (1975). ^{c} R. Prins, *J. Chem. Phys.*, **61**, 2580 (1974). ^{d} R. Prins and T. Novakov, *Chem. Phys. Lett.*, **9**, 593 (1971). ^{e} N. Kosuch, E. Tegeler, G. Wiech, and A. Faessler, *ibid.*, **47**, 96 (1977). ^{f} R. Prins and T. Novakov, *ibid.*, **16**, 86 (1972). ^{g} D. O. Vick, D. G. Woodley, J. E. Bloor, J. D. Allen, Jr., T. C. Mui, and G. K. Schweitzer, *J. Electron Spectrosc. Relat. Phenom.*, **13**, 247 (1978). ^{h} S. Foster, S. Felps, L. C. Cusachs, and S. P. McGlynn, *J. Am. Chem. Soc.*, **95**, 5521 (1973). See also E. Diemann and A. Muller, *Chem. Phys. Lett.*, *19*, 528 (1973). ^{i} These are gas-phase values. They are absolute values and devoid of contact effects. They tend to be high. For example, $I[KNO_3]^j$ = 9.0, $I[Na_3PO_3]^j$ = 10.2, and $I[Tl_2SO_4]^k$ = 9.8 eV. ^{j} R. A. Bowling, J. D. Allen, Jr., and G. K Schweitzer, *J. Electron Spectrosc. 17*, 25 (1979). ^{k} G. K. Schweitzer, A. C. McMurtrie, J. D. Allen, Jr., L. C. Cusachs, D. O. Vick, and G. Finkelstein, *J. Electron Spectrosc. Relat. Phenom.*, **10**, 155 (1977).
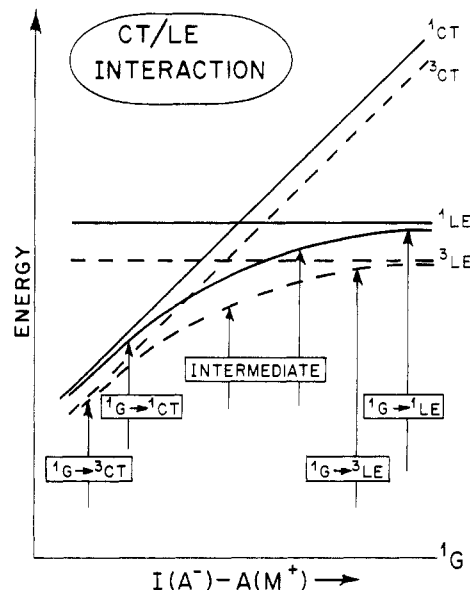

Figure 2. Interaction of $^1CT/^1LE$ and $^3CT/^3LE$ states leading to specification of extreme and intermediate mixing cases.

Figure 2 refers to the situation $a^2 \simeq b^2$, where neither LE nor CT descriptions are appropriate. The middle

TABLE IV. Distinction between ^{1}LE, ^{1}CT $\longleftrightarrow$ ^{1}G, and ^{3}LE, ^{3}CT $\longleftrightarrow$ ^{1}G Transitions[a]

experimental characteristic	$S_1 \longleftrightarrow S_0$	$T_1 \longleftrightarrow S_0$
emission	fluorescence (ns $\leqslant \tau \leqslant \mu$s)	phosphorescence (μs $\leqslant \tau \leqslant$ s)
photoinduced EPR	none	triplet signature
polarization	$\parallel$ to $S_1 \leftarrow S_0$	usually $\perp$ to $S_1 \leftarrow S_0$
absorptivity	large ($10^5 \geqslant \epsilon \geqslant 10$)	small ($10^2 \geqslant \epsilon \geqslant 10^{-4}$)
cation dependence of ϵ and τ	f[A(M$^+$)]	f[A(M$^+$)]; f[ς(M)]$\propto Z^n$, $(4 \geqslant n \geqslant 1)$
anion dependence of ϵ and τ	large effects only with high symmetry anions (e.g., D_{3h}, T_d, etc.)	large effects may occur with any anion, even in C_s

[a] τ is the intrinsic luminescence mean lifetime. ϵ is the absorption crosssection, log $(I_0/I) = \epsilon C l$, where C is concentration (mol/L) and l is the length (cm). The cation dependence ϵ = f[A(M$^+$)] is predicated on Figure 2 where the CT/LE mixing increases as A[M$^+$] gets larger. The Z^n dependence, $\epsilon \propto$ Z(M)^n, $n \leqslant 4$, is the standard atomic number dependence of spin-orbit coupling enhancement effects.[13] The anion dependence of $S_1 \leftarrow S_0$ is predicated on the fact that a large enhancement of ϵ will occur only if the transition is initially (i.e., in the free anion) highly forbidden. Such restrictions do not pertain in the $T_1 \leftarrow S_0$ transition where the only requirement is that spin-orbit coupling can increase.

region is referred to as the intermediate or LE/CT situation.

The description, however, remains inadequate. Both the LE and CT configurations are open shell and, as a result, the wave functions ψ_{LE} and ψ_{CT} must occur in spin-singlet and spin-triplet varieties. These latter states, namely $^3\psi_{LE}$ and $^3\psi_{CT}$, are also shown in Figure 2, but in a very schematic way.[13]

The discussion, as handled so far, is very simple. To make it more complex is not at all difficult! In fact, if the model is to be used for computations, complications mut be introduced.[14] Indeed, the basis set may be enlarged at will to include many excited configurations, involving not only A$^-$ but also M$^+$; various excited CT configurations, including retro-CT (RCT) situations, ψ(M^{2+},A^{2-}); and even doubly excited situations ψ-(M^{*+},A^{*-}), ψ(M$^+$,A^{**-}); etc. Fortunately, the gist of the model is embodied in Figure 2.

4. Color Induction and Classification

As a result of the LE/CT interactions schematized in Figure 2, the system may acquire color by three mechanisms:

(i) A transition $^1\psi_{LE} \leftarrow {}^1\psi_G$, of which at least part lies in the visible region, but which does not induce color because of a very low absorption cross section, may undergo intensity enhancement as a result of CI. The same applies to the $^3\psi_{LE} \leftarrow {}^1\psi_G$ transition.

(ii) A transition $^1\psi_{LE} \leftarrow {}^1\psi_G$ (or $^3\psi_{LE} \leftarrow {}^1\psi_G$) which is of adequate intensity but which, because of a UV location, is not productive of color, may suffer a decrease of energy and move into the visible region as a result of CI.

(iii) A new transition, one of the $^{1,3}\psi_{CT} \leftarrow {}^1\psi_G$ configurational excitation events, may be of sufficiently low energy and sufficiently high cross section.

In any event, there are four transition types with which we must concern ourselves. These are

$$^1\text{LE} \leftarrow {}^1\text{G} \qquad {}^1\text{CT} \leftarrow {}^1\text{G}$$

$$^3\text{LE} \leftarrow {}^1\text{G} \qquad {}^3\text{CT} \leftarrow {}^1\text{G}$$

and they are shown in Figure 2. The actual lowest energy excited state, of course, is some mixture of all four of these limiting cases. However, in the sense of Figure 2, a smooth transformation exists between the actual state and its limiting components. It remains to be seen whether or not this diagrammatic smoothness has any experimental counterpart and whether or not the limiting characteristics of the four transition types

TABLE V. Distinction between LE $\longleftrightarrow$ G and CT $\longleftrightarrow$ G Transitions

experimental characteristic	LE $\longleftrightarrow$ G	CT $\longleftrightarrow$ G
transition energy (TE)	cation independent ~same as free anion	linear in redox potential of cation
solvent dependence of TE	small	large
emissivity[a]	may occur	probably will not occur
Stokes shift[b]	small or zero	large
observability in free anion	possible	impossible

[a] Radiationless transitions of CT $\rightarrow$ G type are enhanced because of strong solute/solvent coupling, and it is not usually expected that the emissive relaxation process can compete. [b] Observability dependent on presence of an emission process.

will be of any use in determining the origin of the color of post-transition-metal salts.

5. Experimental Distinction of Transition Type

The experimental properties of the four limiting transition types are shown in Tables IV and V. Because of the fairly large number of distinguishing characteristics, one ought to be able to determine the operative mode of color induction in most cases.

IV. Experiment

We review the various anion systems in an effort to discern the effective chromogenic mechanism. We divide the anion classes along the point group classification lines suggested in Table III.

1. Bent Triatomic C_{2v} Anions

A. Nitrites

The colors of nitrite salts (Table I) deviate from the color-additivity principle.[6,15] The emission and absorption spectra[16-18] of two salts, one alkali metal, the other a post-transition metal, are shown in Figure 3. The primary differences[16] of absorptivity occur in the 400–500-nm region, which is enhanced by ~10^2. The primary lifetime differences occur in the phosphorescence emission, which is decreased by ~10^2. The absorptivity enhancement is totally responsible for the color of Pb(NO$_2$)$_2$. The change in band shape of the
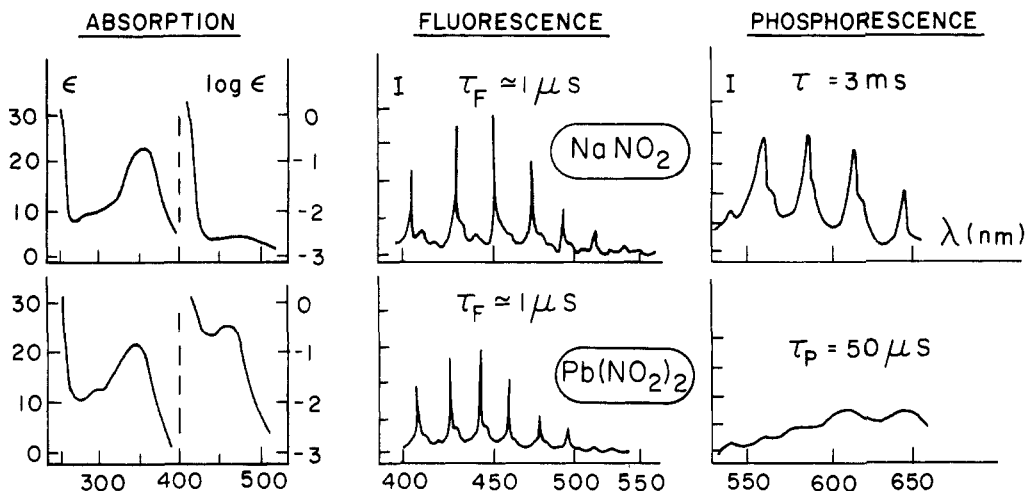
Figure 3. Absorption and emission spectra of $NaNO_2$ (top) and $Pb(NO_2)_2$ (bottom). Absorption refers to solution samples at 295 K. Emission refers to polycrystalline samples of pure salts at 77 K. I denotes emission intensity and ϵ the molar decadic extinction coefficient. Note that the rightmost part of the absorption spectra is in a logarithmic ϵ scaling. τ_F (radiative) and τ_p (total) are luminescence lifetimes (mean) of fluorescence and phosphorescence, respectively.

phosphorescence, which may be real, has not been discussed.

The colors of heavy-metal salts are due to a spin–orbital enhancement of the $T_1 \leftarrow S_0$ transition of the NO_2^- ion.[14,19] The T_1 state is securely identified as $^3B_1(C_{2v}, x \perp NO_2$ plane).[20-24] Absorption and emission spectroscopic data as well as quantum chemical spin–orbit coupling calculations are in full agreement concerning the origins of the color in these sytems. As verification, we present in Table VI the phosphorescence lifetimes of various nitrites as measured directly (τ_p), as calculated from absorption data (τ_p,A), and as computed quantum mechanically (τ_p,Q). The agreement is impressive.

The color induction process, then, is spin–orbit enhancement of $^3LE \leftarrow {}^1G$. The degree of CT mixing is not large because the phosphorescence energy depends only slightly on the nature of the metal cation. Nonetheless, it is this CT mixing of type $^1CT/^3LE$ which enhances spin–orbit coupling and which is responsible for the production of color in the nitrite salts.[14]

The value $I[NO_2^-]$ is certainly among the lowest listed in Table III. Consequently, should $^1CT \leftarrow {}^1G$ transitions ever occur at low energy, they should do so in heavy-metal nitrite salts. In accord with this, a $^1CT \leftarrow {}^1G$ transition of the $AgNa(NO_2)_2$ crystal is observed[23] at 3.1 eV, where it undoubtedly makes its contribution to the color of this system. Furthermore, the $T_1 \rightarrow S_0$ energy exhibits a dependence[18] on metal cation, the maximum varying between 530 and 590 nm in a manner which suggests a moderate variation in the degree of $^3LE/^3CT$ mixing in different nitrite salts.

B. Chlorites

Color among the heavy-metal chlorites is common and quite variable (see Table I). The UV–VIS absorption spectra of aqueous solutions have been reported,[5,25,26] but there is little agreement concerning either spectra or transition assignments. This is hardly surprising because it is very difficult to handle these systems: Many of the heavy-metal salts are only sparsely soluble ($<10^{-3}$ M); decomposition in solution, particularly at high T and low pH, is common;[27] decomposition often generates dissolved ClO_2 gas which

TABLE VI. Phosphorescence Lifetimes of Nitrite Salts (s)[a]

cation	τ_p	τ_p, A	τ_p, Q
Na(I)	$3.3 \times 10^{-3}; y$	3.3×10^{-2}	$2.3 \times 10^{-2}; y$
			$1.76; z$
			$\infty; x$
Ag(I)	1×10^{-4}		$2 \times 10^{-4}; x$
	6×10^{-4}		$6 \times 10^{-4}; y$
	3.5×10^{-3}		$2 \times 10^{-2}; z$
Tl(I)	9×10^{-5}	6×10^{-4}	
Pb(II)	7×10^{-5}	5×10^{-5}	

[a] z is the principal axis (C_{2v}) and x is perpendicular to the NO_2^- plane. The x, y, z notations denote polarization directions (from refs 16–19).

produces[28] an interfering absorption at ~ 360 nm; decomposition precludes growth of good crystals; and, finally, many of the salts (e.g., $AgClO_2$) are photolabile.

Some absorption spectra[29] are shown in Figure 4. Three observations are immediate. First, the absorption spectra, with more or less complete retention of shape, move toward lower energy [i.e., Ag(I) < Cd(II)] in a way which is consistent with increasing electron affinity of the cation. Second, a distinct intensification occurs at long wavelengths, 340–420 nm, for the heavy-metal salts.[30] Third, a weak solvent dependency is observable in the aqueous and alcoholic solvent media.

Color induction in the chlorites, then, is a conjunction of a shift in energy and a spin–orbit perturbation. The former is a result of increasing $A[M^+]$, the latter a straightforward Z effect. However, the energy shifts are sufficiently small that we can, with complete assurance, identify the parental process as $^3LE \leftarrow {}^1G$. Furthermore, this excitation must lie further to the left on Figure 2 than does that for nitrite, and it is this intrusion into the intermediate LE/CT mixing region which is responsible for the energy shifts.

C. Degree of LE/CT Mixing

We now inquire into the degree of CT character in the chlorites. The valence-state ionization energy (VSIE)[7] of Cl is less than that of N and, in addition, ClO_2^- has 20 electrons whereas NO_2^- has only 18. Thus, we expect $I[ClO_2^-] < I[NO_2^-]$. The results of a quantum
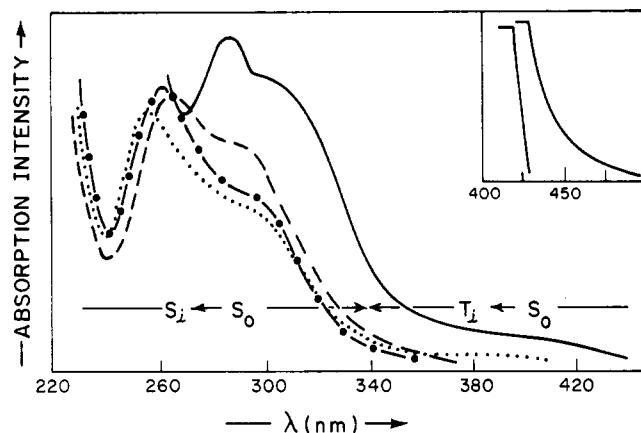
Figure 4. Absorption spectra of chlorite salts at 25 °C: (—) $AgClO_2$ in $AgClO_4$ crystal; $[ClO_2^-] \simeq 5 \times 10^{-3}$ M; (— — —) $NaClO_2$ in ethanol; $[ClO_2^-] \simeq 5 \times 10^{-3}$ M; λ_{max} 265 nm (ϵ 135); (— · — ·) 5×10^{-3} M $NaClO_2$, aqueous; λ_{max} 260 nm (ϵ 160); (· · ·) 4×10^{-3} M $NaClO_2$ in 0.92 M $CdSO_4$, aqueous. Inset: Absorption edge of $Pb(ClO_2)_2$ crystal.
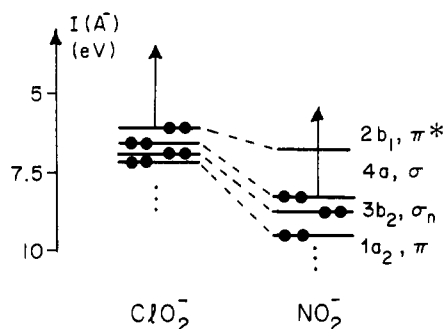
Figure 5. Ionization potentials of ClO_2^- and NO_2^- obtained from an MO calculation using Koopmans' theorem. The orbital from which the electron is ionized is denoted by a vertical arrow. Representation symbols (C_{2v}) and orbital types (n denotes nonbonding, etc.) are also shown. The lowest energy unoccupied MO in ClO_2^- (not shown) is $4b_2;\sigma^*$.

chemical calculation agree (Figure 5) and suggest that ΔI can be as large as 2.5 eV. A similar conclusion follows from Table III, where comparison of the numbers[31] $I[NO_2^-]$ = 5.4 eV and $I[ClO_2^-]$ = 3.3 eV again suggest $\Delta I \simeq 2$ eV. Thus the $^{1,3}CT \leftarrow {}^1G$ transitions of ClO_2^- ion should lie at lower energies than those of NO_2^-, and it is the increased CT/LE interactions which are responsible for the energy shifts of Figure 4 and the photolability and chemical lability of these salts. The ClO_2^- salts systems, in other words, lie in or near the intermediate region of Figure 2.

2. Linear Triatomic $C_{\infty v}$ and $D_{\infty h}$ Anions

The NCO⁻, NCS⁻, and NNN⁻ ions contain 16 valence electrons and have a linear $\tilde{X}^1\Sigma^+$ ground state. The $^{1,3}LE$ states of all these molecules lie in the UV region:[32-35] NCO⁻, 200 and 280 nm; NCS⁻, 230 and 340 nm; and NNN⁻, 240 and >330 nm. Consequently, intensity enhancement of either $^1LE \leftarrow {}^1G$ or $^3LE \leftarrow {}^1G$ will not, of itself, generate color—a concomitant, considerable energy reduction of the $^{1,3}LE$ states is mandatory.

The computed energies, $I[NCO^-]$ = 8.8, $I[NCS^-]$ = 7.9, and $I[N_3^-]$ = 7.7 eV, indicate that $I[NCO^-]$ is slightly greater than $I[NO_2^-]$, which, in turn, is slightly greater than $I[NCS^-]$ and $I[N_3^-]$. Consequently, in view

of the similarity of ionization values, the $^{1,3}CT$ states will lie at approximately the same energy in all four systems. As a result, one expects more CT/LE interaction in the linear triatomics because the LE states lie at higher (i.e., more comparable) energies in these systems. However, it is unlikely that this interaction will lead to excited states of energies less than ~3 eV. That is, these salts are not expected to be colored. The general correctness of these conclusions is validated by such experiment as exists: In source a, Table III, $I[NO_2^-]$ - $I[N_3^-]$ = 0.6 eV, in accord with the computational results cited. And, in accord with prediction, Ba(II), Hg(II), Pb(II), Ag(I), and Tl(I) salts are all colorless, the sole exception being TlN₃ which, reportedly, is yellow.

We emphasize: The same phenomena which typify C_{2v} anions should also occur in $C_{\infty v}$ and $D_{\infty v}$ systems. However, because of confinement to the UV in the latter cases, these phenomena will not be chromogenic.

The lowest energy MO excitation in these molecules is $\pi^* \leftarrow \pi$, and it gives rise to the transitions shown[36] in Figure 6. The ^3LE state is now $^3\Sigma^+$, and it may acquire allowedness only by spin–orbit mixing with $^1\Pi$ states. The lowest energy $^1\Pi$ state in these systems is of $(\pi^* \leftarrow \sigma)/(\sigma^* \leftarrow \pi)$ nature, and, consequently, it is of fairly low intensity (i.e., $\epsilon \sim 1000$). Furthermore, it lies at such high energy that the $^1\Pi-^3\Sigma^+$ interaction gap should not be less than 2 eV. Thus, ST mixing is small, and since there is little singlet intensity to steal, one expects that the $^3\Sigma^+ \leftarrow \tilde{X}^1\Sigma^+$ transition will be of very low cross section and polarized perpendicular to the molecular axis. Since these conclusions are also valid in the MO computational frame, we conclude that the $T_1 \leftarrow S_0$ transition will be very weak unless anion/ cation complexes possess a low-energy CT transition of a symmetry that will mix, under the influence of spin–orbit forces, with $^3\Sigma^+$.

A. Cyanates

Some absorption spectra[32] are given in Figure 7. The development of a weak absorption band at ~280 nm is evident in the heavy-metal salts, as are $^1CT \leftarrow {}^1G$ processes in the 200–260-nm region. The enhancement at ~280 nm is consistent with the assignment $^3\Sigma^+ \leftarrow \tilde{X}^1\Sigma^+$. The cyanate salts exhibit a phosphorescence[35] which is thought to be intrinsic to the NCO⁻ system. The relationship of the ~280-nm absorption and phosphorescence is as follows:

(i) An approximate mirror symmetry exists between them.

(ii) A large Stokes shift of ~7000 cm⁻¹ exists between emission and absorption and is associable, in part anyway, with the fact that $\tilde{X}^1\Sigma^+$ is linear whereas $^3\Sigma^+$ is bent.

(iii) As ϵ increases, τ_p decreases in a consistent fashion, as is illustrated in Table VII.

(iv) The value calculated from MO considerations[32] for NaOCN is τ_p = 130 ms, in good agreement with the observed value, τ_p = 210 ms.

(v) The phosphorescence maxima vary with cation. For example, the maximum for $Pb(NCO)_2$ lies 4000 cm⁻¹ below that of NaOCN. The absorption spectra exhibit similar shifts, in accord with the expected CT/LE mixing.

Thus, while NCO⁻ behaves phenomenologically in the

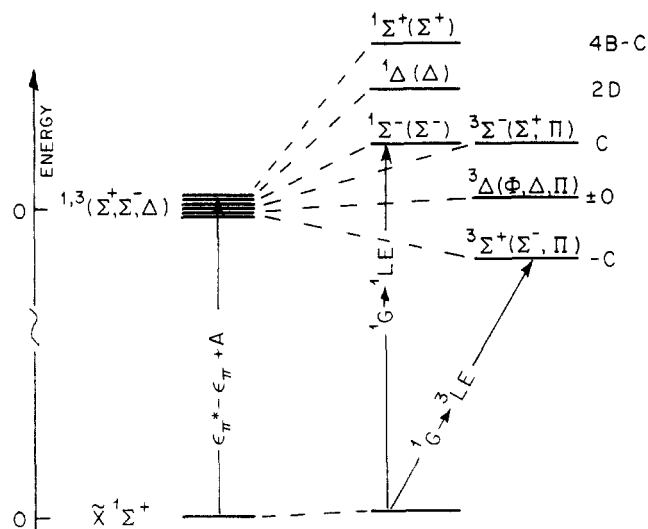**Figure 6.** The ^{1}LE and ^{3}LE states of NCO$^-$ and their MO genesis. The parameters ϵ_π^*, ϵ_π, A, B, C, and D are defined in Wittel et al.[36] The scheme shown here is based on $A \gg B = C = D$. The state symbolics in the upper right are $^{2S+1}\Gamma$ in $C_{\infty v}$ (Γ in $C^*_{\infty v}$, where $C^*_{\infty v}$ is the double group). This same diagram applies to NCS$^-$ and N$_3^-$, with appropriate changes to $D_{\infty h}$ and $D^*_{\infty h}$ in the latter case.

TABLE VII. Extinction Coefficient ϵ [L/(mol cm)] and Phosphorescence Lifetime τ_p (ms) for Cyanates^a

cation	ϵ ($\sim$ 300 nm)	τ_p	$\epsilon/\epsilon_{Na(I)}$	$\tau_{p,Na(I)}/\tau_p$
Na(I)	0.0038	210	$\equiv 1$	$\equiv 1$
K(I)	0.0034	370	0.9	0.6
Cd(II)	0.027	160	7.1	1.7
Hg(II)	0.028	30	7.4	7.0
Pb(II)	0.27	7	71	30

^{a} Since $\epsilon \propto 1/\tau_p$, the last two columns should be identical if the intrinsic radiative process connects the same two states.

Figure 8. Emission spectra of two thiocyanates in aqueous glass (solid line) and in crystal (dotted line) at 77 K. The crystal systems have $\tau_p \simeq 5 \times 10^{-3}$ s, whereas the aqueous systems have $\tau_p \simeq 5 \times 10^{-1}$ s.

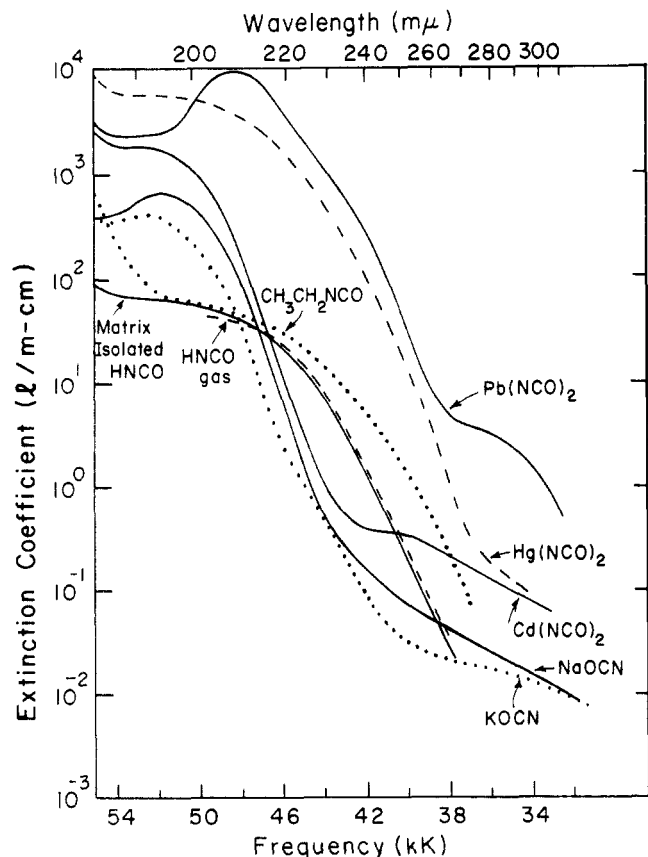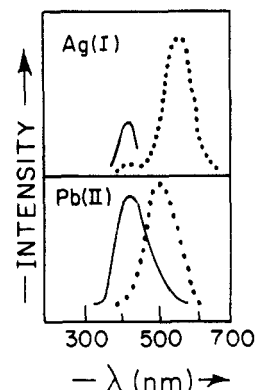**Figure 7.** Absorption spectra of cyanates. The 210-nm process in HNCO and C$_2$H$_5$NCO is ($^1\Sigma^-,^1\Delta) \leftarrow \tilde{X}^1\Sigma^+$. The 280-nm process is $^3\Sigma^+ \leftarrow \tilde{X}^1\Sigma^+$. ^{1}CT $\leftarrow$ ^{1}G transitions are evident in the heavy-metal salts in the region 190–250 nm.

same way as NO$_2^-$, color production does not occur because the ^{1,3}LE $\leftarrow$ ^{1}G transitions lie in the UV region.

B. Thiocyanates

The absorption spectra[33] of the thiocyanates resemble those of the cyanates except that they lie 30 to 50 nm

to lower energy. These compounds also phosphoresce, lifetimes ($\tau_p \sim 0.15$ s) and locations ($\lambda_{max} \sim 420$ nm) being more or less invariant for K(I), Ba(II), Cd(II), and Zn(II). In these systems, T$_1$ is essentially pure ^{3}LE.

The Ag(I) and Pb(II) salts, for which phosphorescence spectra are shown in Figure 8, are exceptional.[33] These salts possess new absorption features at $\sim$260 nm which are undoubtedly of CT nature. Furthermore, the emission spectra of the crystalline and aqueous, glassy systems are different with respect to both λ_{max} and τ_p. We conclude that the ionic form prevails in the aqueous systems whereas a covalent form is certainly present in the crystalline phase. It appears, for the emissive crystalline form, that either CT/LE mixing is considerable or even that the CT state is the lowest energy excited state.

C. Azides

These salts, particularly those of the heavy metals, are both insoluble and dangerous. Both of these characteristics probably indicate considerable covalency and, hence, CT character. However, these same characteristics also ensure that very little work is available for these systems.[34] Neither the light- nor the heavy-metal salts emit. However, the $^1\Sigma_u^- \leftarrow \tilde{X}^1\Sigma_g^+$ transition of N$_3^-$ lies at $\sim$230 nm, and, by analogy with NCO$^-$ and NCS$^-$, one expects the $^3\Sigma_u^+ \leftarrow \tilde{X}^1\Sigma_g^+$ transition to lie at $\sim$340 nm.

Consequently, direct enhancement of ^{3}LE $\leftarrow$ ^{1}G will not be productive of color. However, since $I[N_3^-] \leq I[NCS^-]$, it is possible that CT/LE mixing could move the ^{3}LE state close to or even into the visible region. It is perhaps such a mechanism that underlies the yellow color of the Tl(I) salt.

3. Planar Tetraatomic D_{3h} Anions

The anions NO_3^-, CO_3^{2-}, and BO_3^{3-}, like their neutral isoelectronic counterpart BF_3, are planar and trigonal. The borate ion, as witness the extensive use of boric acid glasses in the early days of molecular luminescence spectroscopy,[37] is essentially transparent at all $\lambda \geq 200$ nm. The carbonate ion[38] exhibits no detectable absorption at $\lambda \geq 250$ nm. The nitrate ion has been studied extensively:[39-42] It exhibits a weak, $\epsilon \simeq 20$, $S_1(\pi^*) \leftarrow S_0(n)$ transition at $\lambda \simeq 300$ nm and a $T_1(\pi^*) \leftarrow S_0(\pi)$ transition with origin at 380 nm, this latter being exceedingly weak for reasons totally analogous to those discussed for the $^3LE \leftarrow {}^1G$ transition of cyanate anion (see Section IV.2). Consequently, a simple enhancement of the intensity of the $^3LE \leftarrow {}^1G$ transitions of these systems will not induce color. Indeed, should either the BO_3^{3-} or CO_3^{2-} systems possess colored heavy-metal salts, we would be forced to conclude that the chromogenic transition was of $^1CT \leftarrow {}^1G$ type. In the case of NO_3^- anion, the matter is less simple because a CT/LE interaction could readily move the 380 nm $^3LE \leftarrow {}^1G$ transition into the visible range where, presuming it had also intensified, it could well be chromogenic.

The experimental[43] ionization energies $I[NO_3^-] = 5.6$ and $I[CO_3^{2-}] = 5.1$ eV are 2.4 and 1.93 V larger, respectively, than the experimental ionization energy $I[NO_2^-] = 3.2$ eV. The value $I[BO_3^{3-}]$ is not known; however, calculations (normalized to the above experimental values for CO_3^{2-} and NO_3^-) suggest $I[BO_3^{3-}] = 4.4$ eV. In view of our experience with nitrite systems (see section IV.1.A), we conclude that all these salts, with the possible exception of the Ag(I), Hg(I), and Au(I) salts, should be colorless, a conclusion which is in full accord with experiment for NO_3^- and CO_3^{2-} salts. Unfortunately, because of the tendency of the borates to form polymeric anions, insufficient data for simple BO_3^{3-} systems are available for inclusion of the borate salts in the above experimental generalization.

The charge-transfer transitions of Fe(III), Ce(IV), and Fe(III) nitrates have been observed, and it has been shown[41] that they correlate linearly with the oxidation/reduction potential $M^{n-} \leftrightarrow M^{(n-1)-}$. By use of this correlation and the data of Figure 1, it is a simple matter to predict that the $^1CT \leftarrow {}^1G$ transitions of the Ag(I), Hg(I), and Au(I) salts should be $AgNO_3$ 280 nm, $HgNO_3$ 300 nm, and $AuNO_3$ 360 nm. Thus, one expects that $AgNO_3$ and $HgNO_3$ will be colorless. On the other hand, one predicts that $AuNO_3$ will be colored, almost certainly yellow, either because of LE/CT mixing followed by an enhancement of intensity and a decrease of energy for the $^3LE \leftarrow {}^1G$ transition or because of intrusion of the low-energy edge of the $^1CT \leftarrow {}^1G$ transition into the visible region. In accord with this, the silver salt is colorless; $Hg_2(NO_3)_2$ solutions are colorless at 77 K but a weak yellow (possibly attributable to the presence of $Hg_2(OH)NO_3$ at 300 K; and $AuNO_3$ is distinctly yellow.

In the carbonates, the $^1CT \leftarrow {}^1G$ transition should lie to lower energy by 0.5 eV relative to the nitrates. Thus, one now expects that all three salts should behave as follows: colorless or weak yellow for Ag_2CO_3; a deep yellow for Hg_2CO_3; and a red-yellow for Au_2CO_3. The observed colors are yellow and yellow-brown for the

TABLE VIII[a]

	cation							
anion	Ba	Ca	Au	Hg	Tl	Pb	Cd	Bi
SO_3^{2-}			ni	ni				ni
ClO_3^-		ni	ni					ni
PO_3^{3-}		ni	ni	ni			ni	ni
BrO_3^-			ni					ni
IO_3^-		ni	ni	yellowish				

[a] The absence of an entry denotes "colorless"; the symbol "ni" denotes "unavailability of information".

Ag(I) and Hg(I) salts, respectively. That for the Au(I) salts is unknown to us.

The nitrate salts exhibit a long-lived luminescence.[44] In the $Hg_2(NO_3)_2$ salt the maximum is at ~ 550 nm whereas in the Tl(I), Ba(II), Bi(II), and Cd(II) salts it lies at ~ 450 nm. The observed red shift of ~ 100 nm agrees with the large $^{1,3}CT \leftarrow {}^1G$ component expected to exist in the lowest excited states of the mercury salt. However, it is not sure that this luminescence is intrinsic.[44]

In sum, then, the observed colors of the carbonate salts are almost surely $^{1,3}CT \leftarrow {}^1G$ in nature. Color should be more common among the simple borates than the carbonates and, where observed, will assuredly be $^{1,3}CT \leftarrow {}^1G$ in nature. The few observed colors of nitrate salts are best represented as $^3(LE/CT) \leftarrow {}^1G$. In all of these cases, however, much further work remains to be done.

4. Nonplanar C_{3v} Anions

The most common oxy anions in this group are SO_3^{2-}, PO_3^{3-}, ClO_3^-, BrO_3^-, and IO_3^-. They contain 26 valence electrons and are essentially uninvestigated.[45] None of them possesses low-energy $^{1,3}LE$ states. In fact, the $^1LE \leftarrow {}^1G$ transitions of ClO_3^- and BrO_3^- lie in the VUV, that of IO_3^- and PO_3^{3-} below 300 nm, and that of SO_3^{2-} below 330 nm. Furthermore, the phosphites and sulfites are so subject to decomposition that we abandoned our own efforts in this area. In any event, color will not be induced by $^{1,3}LE \leftarrow {}^1G$ events or spin–orbit intensification thereof.

The ionization energy data are confusing. Referring to Table III, source b, moderately low energy $^{1,3}CT \leftarrow {}^1G$ transitions are not expected. On the other hand, sources a and c would suggest a situation comparable to nitrite: that is, while the CT states should be of sufficiently low energy to interact strongly with the LE states (because these are of high energy), they are of insufficiently low energy for color induction. In sum, the only system where color phenomena might be expected is iodate. The available information on colors is given in Table VIII.

5. Tetrahedral XO_4^{n-} Anions

The class of tetrahedral inorganic anions is very large. It includes, for example, the species ClO_4^-, BrO_4^-, IO_4^-, SO_4^{2-}, PO_4^{3-}, MnO_4^-, CrO_4^{2-}, VO_4^{3-}, ReO_4^-, TcO_4^-, WO_4^{2-}, MoO_4^{2-}, etc. All of these ions contain 32 valence electrons and are isoelectronic with gaseous OsO_4 and RuO_4. There has been considerable interest in these species: The solid-state physicist has been engrossed with the tungstates, molybdates, phosphates, and va-

nadates because of their technological importance, and the physical chemist has shown an inordinate attachment to chromates and permanganates, perhaps because of their ubiquity and the beauty of their colors. As a result, a good deal of hard information is available.

It is generally agreed[46,47] that the five topmost filled MOs of the T_d entity are 1e, $2t_2$, $2a_1$, $3t_2$, and $1t_1$. Apart from this, virtually all possible permutations of these MOs have been suggested at one time or another. It is also generally agreed that the lowest energy transitions are of an *intraionic CT nature*. That is, an electron which is largely localized on the four oxygen centers of $XO_4{}^{n-}$ is excited[48] to an orbital largely localized on X. We emphasize that, in our terminology, this transition is referred to as "LE" and that only *interionic* transitions are named "CT". In any event, regardless of terminology, it is conceded that the MO diagram of Figure 9 is a good one-electron starting point.

Given the MO diagram (Figure 9), we may assert the following:

(a) Since the 2p oxygen AO energy, with a charge of −0.25 e on each oxygen, is ∼12.5 eV, it seems fair to assert that $I[XO_4{}^{n-}]$ will not usually lie below 9 eV. In accord with this, the ionization potentials of gaseous molecules usually lie at about 10 eV: $I[RuO_4] = 12.09$, $I[OsO_4] = 12.3$, $I[KReO_4] = 10$, $I[MnO_3Cl] = 11.8$ eV,[9] etc. A similar conclusion follows from inspection[49] of source b, Table III. In view of these numbers, one would not expect interionic CT of type

$$M^+ \xrightarrow{e^-} A^-$$
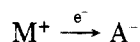
to play a significant role in color induction in these systems.

(b) The lowest-energy transitions will usually be of 2e ← t_1 type. This orbital excitation gives rise to four excited states, $^1T_2$, $^3T_2$, $^1T_1$, and $^3T_1$. It is conceded[47] that the lowest energy allowed transition is of $^1T_2$ ← $^1A_1$ type, (x,y,z)-allowed, and it is generally thought to be responsible for the distinctive low-energy band which characterizes and provides the colors of many of these compounds. The experimental identification of $^1T_1$ ← $^1A_1$ and $^1T_2$ ← $^1A_1$ states is available in a few compounds.[50–55] It is probable that the $^1T_1$, $^3T_1$, and $^3T_2$ states all lie at lower energy than $^1T_2$.

(c) No T_d ion in true solution has been found to emit light. Presumably, this property is enforced by the considerable change of solute/solvent interactions which accompanies the $^{1,3}LE$ ← ^1G excitation and which may lead to energy dissipation in the matrix. However, it is undoubtedly aided by the highly forbidden nature of the $^3T_2$, $^3T_1$ → $^1A_1$ emission processes, the latter, for example, being both spin and orbitally forbidden.

Despite this close connectivity of all T_d anions, we find it difficult to discuss them as a coherent whole. Rather, we find that an appreciable amount of information is available for some of them and little or nothing for many of the others. Furthermore, even for those for which information exists, the type of this information is not identical in all cases. Thus, for MnO_4^-, for example, a great deal of polarized single-crystal absorption spectroscopy is available, and little else. On the other hand, for $WO_4{}^{2-}$, a great deal of luminescence studies are available, and little else. It is such circumstances which force the following compartmentalization.
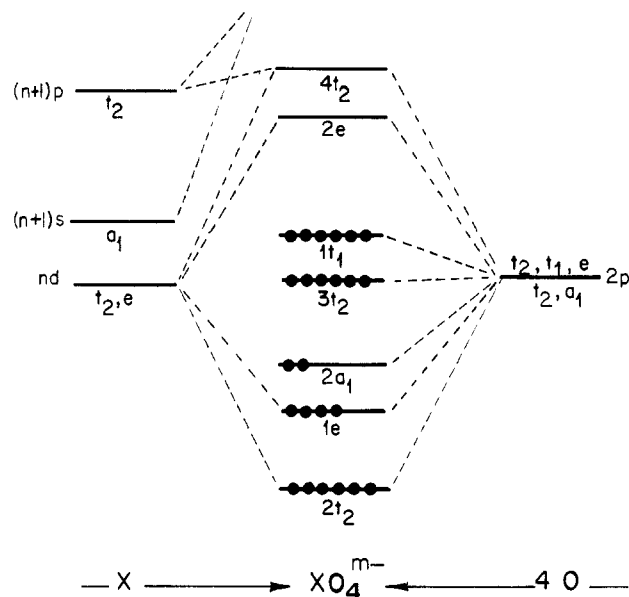

Figure 9. A schematic MO energy level diagram for a 32-electron T_d ion or molecule, $XO_4{}^{m-}$. n denotes the principal quantum number. The $3t_2$ MO usually contains little or no 4d character, and for that reason no compositional connection to nd is shown. A similar comment applies to the (n + 1)s/$2a_1$ compositional connection.

A. Class 1: MnO_4^-, TcO_4^-, ReO_4^-, $CrO_4{}^{2-}$, and $VO_4{}^{3-}$

Of these salts, MnO_4^- and $CrO_4{}^{2-}$ are already colored. Consequently, questions refer not to color induction but rather to its alteration. We shall discuss MnO_4^- in some detail because the phenomena it exemplifies are common.

The electronic structure of MnO_4^- is reasonably well established.[51,52,54,55] The origin band $^1T_2$ ← $^1A_1$ lies at ∼18 200 cm^{-1} and that of $^1T_1$ ← $^1A_1$ at ∼14 300 cm^{-1}. With these energies in mind, the phenomenon of concern, as illustrated in Figure 10, consists of the development of intensity in the 15 000-cm^{-1} region for the solid salts. Since the site symmetry in these salts is no longer T_d but for Li(I) is C_{3v}, for K(I) is C_s, for Ba(II) is C_2, and for Ag(I) is C_1 and since the $^1T_1$ state in each of these site symmetries splits into at least two components, of which at least one component is excitable by dipole-allowed processes from the ground-state $^1A_1$, it is reasonable to suppose that this splitting leads to site-symmetric induction of allowedness into the originally forbidden $^1T_1$ ← $^1A_1$ transition.[56]

This interpretation, totally feasible in Li(I), K(I), and Ba(II) salts, becomes somewhat untenable in the Cs(I) salt, where diminution of intensity of $^1T_2$ ← $^1A_1$ seems to occur, and is almost totally untenable in the Ag(I) salt, where the $^1T_2$ ← $^1A_1$ intensity seems to have more or less disappeared. In the latter case, one must not only explain the appearance of intensity in the 15 000-cm^{-1} region, one must also explain its disappearance in the 20 000-cm^{-1} region. The simplest interpretation invokes a splitting of $^1T_2$ so that one (or two) components moves to lower energy (i.e., to 14 000 cm^{-1}), and one (or two) moves to higher energy (i.e., to 20 000 cm^{-1}).

In any event, the intensification in the 15 000-cm^{-1} region cannot be the result of a
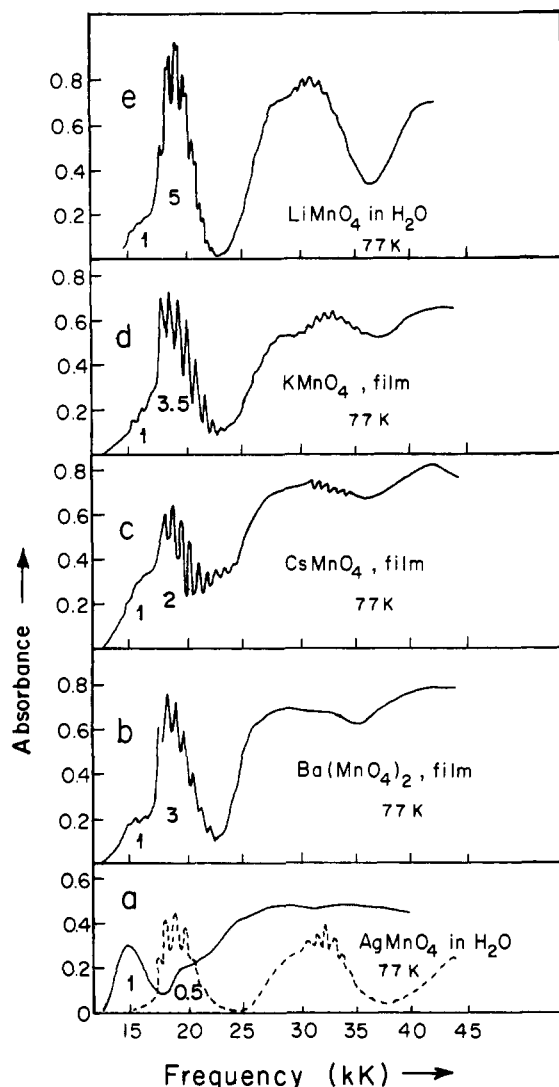
$$MnO_4^- \xleftarrow{e^-} M^+$$
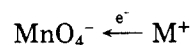
Figure 10. Absorption spectra of permanganates. The dashed line spectrum in (a) is that of the MnO_4^- ion. It refers to a dilute aqueous solution of $AgMnO_4$ at 293 K. Upon cooling of this solution to 77 K, microcrystals of $AgMnO_4$ form, and the spectrum becomes that of the solid line in (a). The extinction coefficient for MnO_4^-, $\epsilon \simeq 2.4 \times 10^3$ at 19000 cm^{-1}, does not alter much upon crystallization to $AgMnO_4$, $\epsilon \simeq 3 \times 10^3$ at 15000 cm^{-1}. However, the shift of ~5000 cm^{-1} produces a striking color change from the red purple characteristic of MnO_4^- ion to a bright green characteristic of a microcrystalline suspension. These changes (and spectra) are totally reversible with temperature. The color of a concentrated $AgMnO_4$ solution at 77 K is the dark violet color characteristic of the bulk single crystal. The spectra e, d, c, and b refer to thin solid films of $LiMnO_4$, $KMnO_4$, $CsMnO_4$, and $Ba(MnO_4)_2$, respectively, which were deposited from aqueous solution on quartz plates. All of these spectra exhibit the standard MnO_4^- ion spectrum. However, they also exhibit a long-wavelength component. The more intense this long-wavelength component, the less intense is the ion spectrum. It is clear that the 15000-cm^{-1} component does not refer to the ion but to some sort of metal/ion associate and that the formation of this associate increases in the order Li < K < Cs. The numbers on the graphs give the ratios of intenity, $\mathcal{J}$ (15000 band)/$\mathcal{J}$ (20000 band). In $AgMnO_4$, these numbers refer only to the solid curve.

RCT transition[57] or of a

$$M^+ \xleftarrow{e^-} MnO_4^-$$
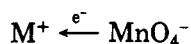
CT transition. The absorption energies exhibit too small an alteration to render any such interpretations feasible.

The $^1T_1 \leftarrow {}^1A_1$ splitting/intensification, then, is held

responsible for the alteration of the color of MnO_4^- salt crystals: K(I), purple; Na(I), black; Cs(I), black; Ag(I), blue-black in bulk, green in thin layers; and Zn(II), dark blue. Parallel phenomena in CrO_4^{2-} salts (e.g., Ag(I), brick red; K(I), yellow; etc.) are interpreted in a similar vein.[58,59] Indeed, it is probable that the color changes brought about by acidification of chromate salt solutions is of like nature and attributable to the decrease of symmetry associated with the transformation $CrO_4^{2-} \rightarrow HCrO_4^-$.

The $^1T_2 \leftarrow {}^1A_1$ transitions of ReO_4^-, VO_4^{3-}, and TcO_4^- lie at 43.7×10^3, 36.9×10^3, and 34.6×10^3 cm^{-1}, respectively.[60-62] Consequently, it is unlikely that the effects discussed above, although undoubtedly present, will have significance in terms of either color induction or color alteration.

The $^3T_1$ and $^3T_2$ states of MnO_4^- should also lie in or near the 15000-cm^{-1} region,[63] and there has been some discussion concerning the observability of these levels in chromates,[64] vanadates,[65] and dichromates.[66] Whether or not symmetry decrements and heavy-atom effects lead to intensification of triplet $\leftarrow$ singlet transitions in the specific case of the permanganates and whether or not such effects contribute to the 15000-cm^{-1} phenomenology in Figure 10, we cannot say. However, there seems no reason why they should not. In fact, we now discuss a class of T_d molecules in which the triplet $\rightarrow$ singlet transitions constitute the dominant observables.

B. Class 2: WO_4^{2-}, MoO_4^{2-}, and VO_4^{3-}

Tungstate, molybdate, and vanadate[65] ions luminesce in the solid phase.[67-73] They also serve as efficient sensitizers for the fluorescence of rare-earth dopants.[67,74,75] The observed emission appears not to be of defect, impurity, or band type, but to be an intrinsic, molecular, radiative relaxation of the oxy anion.[67,72,76]

The absorption and emission spectra of some molybdates[76] are shown in Figure 11. The energies of neither absorption nor emission maxima correlate with metal redox potentials, and, therefore, these bands are neither CT nor RCT in nature. By default, then, we conclude that they are intrinsic to MoO_4^{2-}.

The absorption intensity, ϵ, at the maximum of the weak absorption band is Na(I) = 1.5, Cd(II) = 14, and Pb(II) = 7. These values suggest either a strongly allowed triplet $\leftarrow$ singlet or strongly forbidden singlet $\leftarrow$ singlet transition. We choose the latter for the following reasons: (a) The extinctions quoted are based on total molybdate present and not on that fraction of it which is involved in whatever complex or associate is productive of this absorption event. Consequently, the values of ϵ are minimal. The correct values could be much larger. (b) The values for the tungstates are considerably higher, that for $PbWO_4$, for example, being $\epsilon = 200$. This value almost surely decrees a singlet $\leftarrow$ singlet transition. (c) There happens to be a low-energy $^1T_1 \leftarrow {}^1A_1$ assignment available which, because it is not assigned to any other transition, is eminently satisfactory for the 300-nm feature (see section V.5.A).

The emission event is almost certainly not inverse to the 300-nm absorption event. First, as is evident in Figure 11, the Stokes shift is very large, being ~10000 cm^{-1} in some cases. Second, the emission excitation spectra[76] exhibit longer wavelength components than
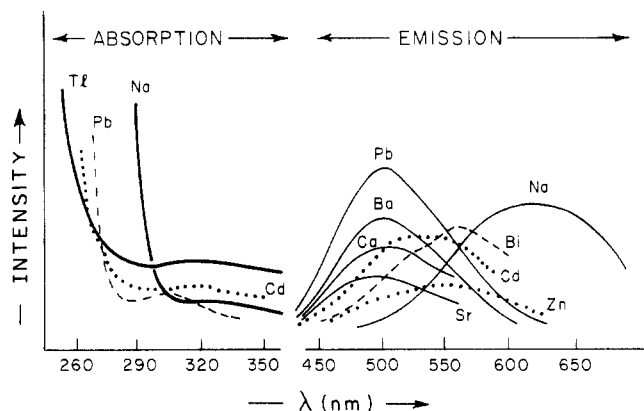
Figure 11. Absorption (300 K, aqueous solution) and emission (77 K, single crystal) of various molybdate salts. The higher energy absorption edges are onsets of intense singlet ← singlet absorption intensity of the anion, λ_{max} 227 nm. The variation of absorption edge is largely attributable to the different concentrations required to observe the weak side bands in the 250–350-nm region. The behavior of the tungstates is very similar except that maxima occur 30–50 nm to higher energy.

TABLE IX. Excitation and Lifetime Data for Molybdate Emission Spectra[a]

cation	excitation spectrum, (λ_{max}, nm)	lifetime, 77 K, (τ, μs)
Li(I)	328	10
Na(I)	325	880
Ca(II)	305	220
Zn(II)	294	36, 30, 44
Sr(II)	245	156
Cd(II)	337	230
Pb(II)	359	10

[a] From ref 76.

are evident in the absorption spectra. Some of the excitation maxima are collected in Table IX, where the long-wavelength extension caused by going from absorption to excitation detection is quite obvious. Third, diffuse reflectance spectra[76] of crystals exhibit the same red extension which is evident in emission excitation. Consequently, there is no doubt that other, very much weaker transitions lie at lower energy than those sampled in the solution absorption spectrum. Furthermore, it appears that the emission process is the inverse of these lower energy absorptive events.

The emissive act appears to be a phosphorescence (i.e., triplet → singlet) event. First, some of the lifetimes (see Table IX) are simply too long ($\sim 10^{-4}$ s) to be interpreted as singlet → singlet. Second, the temperature dependencies of the few lifetimes which have been investigated all exhibit a characteristic behavior:[70,72,77] They plateau at ~ 77 K, and, thereafter, slowly increase to $\tau > 10^{-4}$ s for $T < 77$ K. These effects suggest a temperature inhibition of degradative pathways. Third, the lifetime of a given molybdate is almost always greater than that of the corresponding tungstate[76] and, very often, the heavier the cation, the shorter the lifetime. The clarity of these last observations is somewhat obscured by the effects of trapping levels, methods of sample preparation and crystal growth, impurities, etc.[72] Nonetheless, they are totally consistent with the external heavy-atom effects on a triplet → singlet event. Fourth, and finally, a value $10^{-4} \leq \tau \leq 10^{-3}$ s is reasonable for a phosphorescence process in a molecule which contains heavy atoms such as Mo or W. Con-
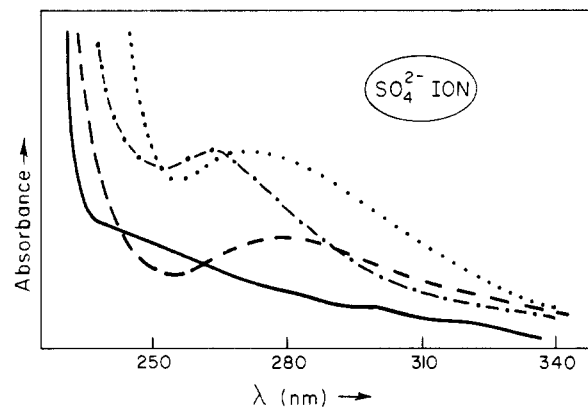

Figure 12. Absorption spectra of some sulfate salts illustrating development of a weak absorption band in the 280-nm region. The apparent absorption edge at ~ 225 nm is intrinsic to Ag^+. (—) Ag_2SO_4 doped into $LiKSO_4$; single crystal, 298 K. Upon cooling to 77 K, the absorption intensity appears to increase, but no increase in resolution is observed. (— — —) $Ag_2SO_4/AgNO_3$, saturated aqueous solution, 298 K. (— · — ·) Ag_2SO_4, saturated aqueous solution, 298 K. (···) Ag_2SO_4 saturated with Na_2SO_4, aqueous solution, 298 K.

sequently, we assign the emission event as either $^3T_1 \rightarrow {}^1A_1$ or $^3T_2 \rightarrow {}^1A_1$.

The tails of the weak absorption events in the molybdates straggle into the visible region and, in sufficient sample thickness, produce a yellow color. It is this effect which we think to be responsible for the yellow color so common among molybdates (e.g., Ag(I), Ce(I), Pb(II), etc.). By the same token, because of their blue shift of 30–50 nm, the tungstates, in agreement with experience, should not usually be colored. A similar statement applies to the vanadates.

C. Class 3: $SO_4{}^{2-}$ and $PO_4{}^{3-}$

The onset of absorption in sulfate salts is usually supposed to occur[78,79] at ~ 200 nm. However, a weak transition may also be observed at 270 nm, and a long tail which extends to much lower energy is also commonly present.[76] Some sulfate absorption spectra are shown in Figure 12. The intensity and energy of this transition are sensitive to salt concentration and to relative anion/cation concentrations. Obviously, the degree of anion/cation association has a large effect on transition probability characteristics.

The extinction coefficient of this band, in especially favorable cases, can be as high as $\epsilon \simeq 600$ L/(mol cm). Consequently, we conclude that this transition is singlet ← singlet, probably $^1T_1 \leftarrow {}^1A_1$ of T_d, possibly split and made allowed by association as in the class 1 and 2 molecules.

6. Salts of Carboxylic Acids

The $^3LE \leftarrow {}^1G$ transition is of $\pi^* \leftarrow n$ type in the oxalates, the origin band being at 327 nm in oxalic acid.[80] The corresponding origins lie[81] at 361 and 341 nm in benzoic acid and phenylacetic acid, respectively, and are of $\pi^* \leftarrow \pi$ type. Neither the nature nor the location of the $^3LE \leftarrow {}^1G$ transition in either formates or acetates is known with any certainty.[81,82] However, it appears that the transition is of $\pi^* \leftarrow \pi$ nature, and it is certain that the origin band lies at $\lambda < 350$ nm. The $^3LE \rightarrow {}^1G$ luminescences of these systems are shown in
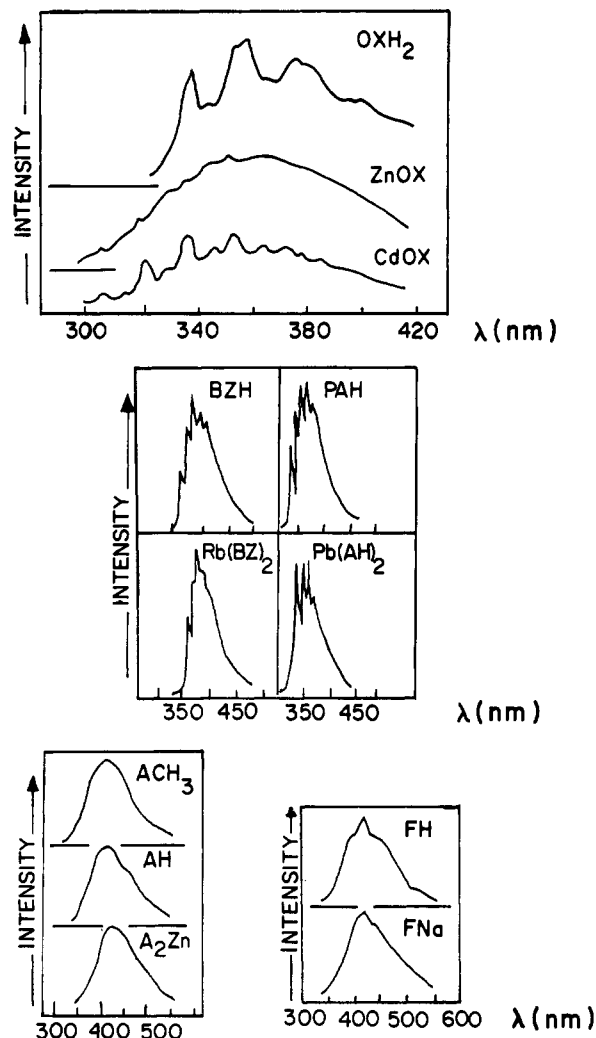
Figure 13. Phosphorescence spectra of carboxylic acids, esters, and salts. The notation is as follows: OX, oxalate, $(COO)_2$; BZ, benzoate, C_6H_5COO; PA, phenylacetate, $C_6H_4CH_2COO$; A, acetate, CH_3COO; and F, formate, HCOO. All spectra were run at 77 K. All spectra, with the exception of those of ZnOX and CdOX (which were microcrystalline), were obtained from glassy solutions.

Figure 13 and, with some exceptions, are in full accord with the absorption spectroscopic data. The exceptions, in all instances, are readily understood in terms of either geometric differences[80,82] between the ^3LE and ^1G states and/or crystalline defects.[80]

The occurrence of color in any of these systems, at least insofar as it is conditioned by a $^3LE \leftarrow ^1G$ absorption mechanism, requires both a large increase ($\times 10^2$, at least) of cross section and a large decrease (0.6 eV, at least) of energy. This latter red shift is so large that it mandates the presence of low-energy $^{1,3}CT \leftarrow ^1G$ transitions and, thereafter, extensive $^3CT/^3LE$ mixing in order to produce the necessary intensification and red shift of the $T_1 \leftarrow S_0$ transition. Since we deem this unlikely (vide infra), we conclude that color conditioned by $^3LE \leftarrow ^1G$ events should be most improbable.

The next question concerns the location of the $^{1,3}CT$ states and the possibility of color induction by one or both of the transitions $^{1,3}CT \leftarrow ^1G$. Unfortunately, no experimental information on $I[A^-]$ is available and, again, we must have recourse to computation. Various computations[83,84] for HCOO$^-$ and comparisons[85] of the "isoelectronic" sequence HCOO$^-$, NO$_2^-$, and O$_3$ suggest

TABLE X. Phosphorescence Lifetimes of Carboxylates[a,b]

cation	anion	n	τ_p, s
Na(I)	benzoate	0	1.68
Cd(II)	benzoate	0	0.38
Ag(I)	benzoate	0	7×10^{-2}
Pb(II)	benzoate	0	2×10^{-2}
Pb(II)	phenylacetate	1	1×10^{-2}
Pb(II)	phenylpropionate	2	4×10^{-2}
Pb(II)	phenylbutanoate	3	~ 1

[a] From ref 81. [b] The value of n is taken from the anion formula $C_6H_5(CH_2)_nCOO^-$. Thus, as n increases, the Pb(II) ion moves further away from the phenyl group on which the $\pi^* \leftarrow \pi$ transition is largely localized.

that the lowest ionization potential of HCOO$^-$ is comparable to but somewhat larger than that of NO$_2^-$. Hence, arguing by analogy with the nitrite systems, one would not expect color of CT origins to be a prominent characteristic of carboxylate salts. Indeed, color, if it occurred at all, should be restricted to the gold salts (Figure 1), with some assurance that it should not occur even there.

In agreement with the above, no salt, including those of Ag(I), Pb(II), Tl(I), Hg(I), of formic, acetic, oxalic, benzoic, or phenylacetic acid is colored. There is no information available, unfortunately, for the Au(I) salts. It should be possible, however, to prepare salts which are colored. For example, many of the carboxylic acids of polynuclear hydrocarbons have $^3LE \leftarrow ^1G$ transitions which lie in the visible region, and the heavy-metal salts of these systems should, indeed, possess color. Unfortunately, again, pertinent information is not at hand.

The same phenomena which characterize nitrites should also be evident in the carboxylates, but should be restricted to the UV region. It is important to demonstrate this correspondence. First, such a demonstration would bolster the thesis of this work simply because heavy-atom spin–orbit effects are not only well-known but even commercially important in the organic domain; second, one can invoke the ingenuity of the organic chemist in order to induce qualitatively new phenomena. That the same phenomena do indeed occur is amply demonstrated in Table X. Compare, for example, the first four entries of Table X with Tables VI and VII. The appearance of a new phenomenon is contained in the last four lines of Table X: a proximity effect, which depends on the distance between the metal ion and the locus of the $^3LE \leftrightarrow ^1G$ transition which it must perturb, is clearly evident.

The heavy-atom effects described here for the carboxylic acids are well-known in the case of the amino acids[86] (and proteins[86]) and the nucleic acids[87] (and RNA and DNA[88,89]), where the observed effects can be either biologically harmful or useful, depending on context. A similar role in photochemistry is well-known. Indeed, the formerly important role of lead tetraethyl "antiknocks" is almost certainly a simple example of a heavy-atom spin–orbit coupling effect on either one or both of the initiation and termination reactions of gasoline combustion.

V. Conclusion

Deviations from the principle of color additivity have been explained by invoking three effects: (i) enhancement of triplet $\leftarrow$ singlet transitions by external

heavy-atom effects; (ii) reduction of symmetry and consequent intensity enhancement of forbidden singlet ← singlet transitions of highly symmetric anions; and (iii) the occurrence of low energy $^{1,3}CT \leftarrow {}^{1}G$ transitions of type

$$M^+ \xleftarrow{e^-} A^-$$
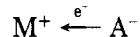
when $I[A^-] - E[M^+]$ is small.

Effect i is the dominant effect in most of the systems investigated. Effect ii appears to be important in some tetrahedral systems. Effect iii contributes in three ways: It provides the dominant channel for spin–orbit mixing of singlet character into triplet states, it produces shifts of $^{1,3}LE$ states to lower energies, and, in some instances, it may be of low enough energy to be directly productive of color.

A primary import of this work is its stark demonstration of the poor state of affairs of the particular area of inorganic chemistry with which it deals. Experimental data, even data of a most primitive sort, are in very short supply. Furthermore, the area is very lean on concepts. Indeed, had this not been the case, the simple ideas presented here would not have sufficed to introduce order or to prosecute review.

All the discussion of this work is based on the idea of an LE/CT mixing which is totally confined to excited states. Such a restriction is wrong, if for no other reason than that it excludes LE/CT/G mixing and eliminates stabilization of anion/cation associates by other than electrovalent forces. This is a serious exclusion, for without orbital extension from anion to cation and/or vice versa (i.e., without some small degree of covalency) all CT ← G transitions will have zero cross section, and, hence, most of the intensity-induction mechanisms which we suppose to be operative will be of no avail. The truth of the matter, however, is that while we certainly invoke CT/LE/G mixing, we refrain from discussing it. To discuss CT/G mixing at this stage would be superfluous: To put it simply, little or no data on associate types, stoichiometries, or stabilities exist for solutions of these salt types, and there seems no point in introducing quantities for which no experimental review is possible.

VI. References

(1) P. R. von Bichowsky, J. Am. Chem. Soc., 40, 500 (1918).
(2) K. Pitzer and J. H. Hildebrand, J. Am. Chem. Soc., 63, 2472 (1914).
(3) C. K. Jorgensen, Mol. Phys., 4, 235 (1961).
(4) C. S. J. Phillips and R. J. P. Williams, "Inorganic Chemistry", Vol. 2, Oxford University Press, 1966, p 498.
(5) N. Konopik, J. Derkosch, and E. Berger, Monatsh. Chem., 84, 214 (1953).
(6) S. P. McGlynn in "Luminescence of Crystals, Molecules and Solutions", F. Williams, Ed., Plenum, New York, 1973, p 399 ff; Izv. Akad. Nauk. SSSR, Ser. Fiz., 37, 546 (1973).
(7) The phrasing used here is embedded in the composite molecule method (CMM): S. P. McGlynn, L. G. Vanquickenborne, M. Kinoshita, and D. G. Carroll, "Introduction to Applied Quantum Chemistry", Holt, Rinehart and Winston, New York, 1972.
(8) A simple enhancement of $S_1 \leftarrow S_0$ absorptivity, without any concomitant energy shift, cannot produce the observed color effects in these salts.
(9) E. Diemann, E. L. Varith, and A. Müller, Chem. Phys. Lett., 51, 460 (1977). MnO$_3$Cl, being gaseous, exhibits minimal contact effects.
(10) H. Hsu, C. Peterson and R. M. Pitzer, J. Chem. Phys., 64, 791 (1976).
(11) S. Nagakura and J. Tanaka, J. Chem. Phys., 22, 236 (1954); S. Nagakura, ibid., 23, 1411 (1955); N. Mataga, Bull. Chem. Soc.

Jpn., 36, 1607 (1963); M. Godfrey and J. N. Murrell, Proc. R. Soc. London, Ser. A, 278, 57, 64 (1964); see also ref 7.
(12) R. S. Mulliken and W. B. Person, "Molecular Complexes", Wiley-Interscience, New York, 1969, Chapter 3.
(13) S. P. McGlynn, T. Azumi, and M. Kinoshita, "Molecular Spectroscopy of the Triplet State", Prentice-Hall, Englewood Cliffs, NJ, 1969.
(14) T. P. Carsey and S. P. McGlynn, J. Am. Chem. Soc., 101, 1728 (1979).
(15) Deviations occur in true solutions as well as in the solid. In the former case, definite stoichiometric complexes of Ag$^+$ and NO$_2^-$ are known.[16]
(16) H. J. Maria, A. Wahlborg, and S. P. McGlynn, J. Chem. Phys., 49, 4925 (1968).
(17) S. Makishima, T. Tomitsu, M. Hirata, S. Hayakawa, K. Hasegawa, R. Kambe, and S. Shionoya in "Luminescence of Organic and Inorganic Materials", H. P. Kallmann and G. M. Spruch, Eds., Wiley, New York, 1962, p 443.
(18) H. J. Maria, A. T. Armstrong, and S. P. McGlynn, J. Chem. Phys., 48, 4694 (1968).
(19) L. E. Harris, H. J. Maria, and S. P. McGlynn, Czech. J. Phys., B5, 654 (1970); B20, 1007 (1970).
(20) R. M. Hochstrasser and H. P. Marchetti, J. Chem. Phys., 50, 1727 (1969).
(21) W. C. Allen and R. N. Dixon, Trans. Faraday Soc., 65, 1168 (1969).
(22) H. J. Maria, A. T. Armstrong, and S. P. McGlynn, J. Chem. Phys., 50, 2777 (1969).
(23) L. E. Reznik and L. M. Rumyantseva, Opt. Spectrosk., 39, 895 (1975) (Engl. Transl., 509); L. E. Reznik, P. R. Garber, and A. E. Fesun, Fiz. Tvert. Tela., 15, 3280 (1973) [Sov. Phys. Sol. State, 15, 2185 (1974)]; L. E. Reznik and P. R. Garber, Opt. Spectrosk., 34, 418 (1973) (Engl. Transl., 237).
(24) S. E. Clark and D. S. Tinti, Chem. Phys. Lett., 60, 292 (1979).
(25) H. L. Friedman, J. Chem. Phys., 21, 319 (1953).
(26) O. M. Lifentsev, Nauch-Issted. Tr. Ivanov. Nauch-Issted. Int. Klopchatobum. Prom., 28, 149 (1966); Chem. Abstr., 68, 13967 (1968).
(27) J. F. White, M. C. Taylor, and G. P. Vincent, Ind. Eng. Chem., 34, 782 (1942).
(28) S. P. Tandon and K. Tandon, Ind. J. Pure Appl. Phys., 7, 245 (1969).
(29) T. P. Carsey, Ph.D. Dissertation, Louisiana State University, Baton Rouge, LA, 1977, p 163.
(30) For example, an aqueous solution of 4×10^{-3} M NaClO$_2$ in 0.92 M CdSO$_4$ absorbs 10% more strongly at 260 nm than a solution containing only the NaClO$_2$, indicating Cd/ClO$_2$ complex formation of some kind (see Figure 4). If now the chlorite concentration of the pure aqueous system is increased by 20% so that absorptivity of the latter is ~10% higher at 260 nm than the NaClO$_2$/CdSO$_4$ system (see Figure 4), an isosbestic point appears at ~320 nm, and it is the absorptivity of the NaClO$_2$/CdSO$_4$ system which is considerably higher at ~380 nm. This intensification is particularly obvious in the AgClO$_4$:AgClO$_2$ crystal.
(31) Sources a and c used comparable experimental techniques. Source b used an independent calibration technique.
(32) J. W. Rabalais, J. R. McDonald, and S. P. McGlynn, J. Chem. Phys., 51, 5103 (1969).
(33) J. W. Rabalais V. M. Scherr, and S. P. McGlynn, J. Chem. Phys., 51, 1723 (1969).
(34) J. R. McDonald, J. W. Rabalais, and S. P. McGlynn, J. Chem. Phys., 52, 1332 (1970).
(35) J. W. Rabalais, J. R. McDonald, and S. P. McGlynn, J. Chem. Phys., 51, 5095 (1969).
(36) S. P. McGlynn, K. Wittel, and J. L. Meeks, "The Chemistry of Cyanates and Thiocyanates", S. Patai, Ed., Wiley, New York, pp 1–68.
(37) M. Kasha, J. Opt. Soc. Am., 38, 1068 (1948).
(38) T. H. Brayden, Jr., Ph.D. Dissertation, Louisiana State University, Baton Rouge, LA, 1968.
(39) E. V. Sayre, J. Chem. Phys., 31, 73 (1959).
(40) S. J. Strickler and M. Kasha, "Molecular Orbitals in Chemistry, Physics, and Biology", P.-O. Löwdin and B. Pullman, Eds., Academic Press, New York, 1964, pp 241–261.
(41) H. J. Maria, J. R. McDonald, and S. P. McGlynn, J. Am. Chem. Soc., 95, 1050 (1973).
(42) R. A. Palmer and M. C.-L. Tang, Chem. Phys. Lett., 31, 492 (1975).
(43) These values are from source b, Table III. We prefer these values to those of source a simply because the differences in the values of I are in closer correspondence with the results of MWH calculations.
(44) H. J. Maria, B. N. Srinivasan, and S. P. McGlynn, "Molecular Luminescence", E. C. Lim, Ed., W. A. Benjamin, New York, 1969.
(45) Much of the spectroscopic work refers to CTTS absorption studies. See, for example, S. P. Tandon and K. Tandon, Ind. J. Pure Appl. Phys., 8, 199 (1970), and E. Hayon, A. Treinin,

and J. Wilf, *J. Am. Chem. Soc.*, **94**, 47 (1972). For photoelectron spectroscopic data, see Table III. For thermodynamic data, see K. H. Stern, *J. Phys. Chem. Ref. Data*, **3**, 481 (1974).

(46) M. Wolfsberg and L. Helmholtz, *J. Chem. Phys.*, **20**, 837 (1952).

(47) C. J. Ballhausen and A. D. Liehr, *J. Mol. Spectrosc.*, **2**, 342 (1958).

(48) S. P. McGlynn and M. Kasha, *J. Chem. Phys.*, **24**, 481 (1956).

(49) The ionization energies in sources *a* and *c*, Table III, vary considerably relative to those in source *b*. Nonetheless, all values are so high for the T_d systems that one would not expect low-energy CT transitions.

(50) J. C. Collingwood, P. Day, R. G. Denning, D. J. Robbins, L. DiSipio, and L. Oleari, *Chem. Phys. Lett.*, **13**, 567 (1972).

(51) C. J. Ballhausen and I. Trabjerg, *Mol. Phys.*, **24**, 689 (1972).

(52) S. L. Holt and C. J. Ballhausen, *Theor. Chim. Acta*, **7**, 313 (1967).

(53) J. C. Duinker and C. J. Ballhausen, *Theor. Chim. Acta*, **12**, 325 (1968).

(54) L. W. Johnson, E. Hughes, and S. P. McGlynn, *J. Chem. Phys.*, **55**, 4476 (1971).

(55) L. W. Johnson and S. P. McGlynn, *J. Chem. Phys.*, **55**, 2985 (1971); *Chem. Phys. Lett.*, **10**, 595 (1971).

(56) As an example, if the site symmetry were S_4, the crystal field would split T_1 into $E \oplus A$ and, since $^1E \leftarrow {}^1A$ is allowed, the increased intensity in the 15 000-cm^{-1} region could be associated with $^1E \leftarrow {}^1A$ in an S_4 site symmetry.

(57) Jorgensen [C. K. Jorgensen, *Acta Chem. Scand.*, **17**, 1034 (1963)] proposed that the

$$CrO_4^- \xleftarrow{\ e^- \ } Ag^+(4d)$$

RCT transition was responsible for a similar effect in $AgCrO_4$ salts.

(58) L. W. Johnson and S. P. McGlynn, *Chem. Phys. Lett.*, **7**, 618 (1970).

(59) D. J. Robbins and P. Day, *Mol. Phys.*, **34**, 893 (1977).

(60) A. Müller and E. Diemann, *Chem. Phys. Lett.*, **9**, 369 (1971).

(61) P. Mullen, K. Schwochau, and C. K. Jorgensen, *Chem. Phys. Lett.*, **3**, 49 (1969).

(62) N. Bailey, A. Carrington, K. A. K. Lott, and M. C. R. Symons, *J. Chem. Soc.*, 290 (1960).

(63) C. J. Ballhausen, *Theor. Chim. Acta*, **1**, 285 (1963).

(64) V. Miskowski, H. B. Gray, and C. J. Ballhausen, *Mol. Phys.*, **28**, 729 (1974).

(65) H. Ronde and G. Blasse, *J. Inorg. Nucl. Chem.*, **40**, 215 (1978).

(66) G. Blasse, *Chem. Phys. Lett.*, **63**, 441 (1979).

(67) F. A. Kroger, "Some Aspects of the Luminescence of Solids", Elsevier, New York, 1948.

(68) C. C. Vlam, *Physica*, **15**, 609 (1949).

(69) C. B. Beard, W. H. Kelly, and M. L. Mallory, *J. Appl. Phys.*, **33**, 144 (1962).

(70) D. Hahn and K. Lertes, *Z. Phys.*, **169**, 331 (1962).

(71) B. I. Maksakov, A. M. Morozov, and N. G. Romanova, *Opt. Spectrosc.*, **14**, 166 (1963).

(72) M. Treadway and R. C. Powell, *J. Chem. Phys.*, **61**, 4003 (1974).

(73) W. V. Loo, *Phys. Stat. Sol. A*, **A28**, 227 (1975).

(74) A. K. Levine and F. C. Patilla, *Appl. Phys. Lett.*, **5**, 118 (1964).

(75) M. Aia, *J. Electrochem. Soc.*, **114**, 367 (1967).

(76) T. P. Carsey, Ph.D. Dissertation, Louisiana State University, Baton Rouge, LA, 1977, pp 164–198.

(77) V. Schafer, *Z. Phys.*, **166**, 429 (1962).

(78) E. Rabinowitch, *Rev. Mod. Phys.*, **14**, 112 (1942).

(79) J. L. Weeks, G. M. A. C. Meaburn, and S. Gordon, *Radiat. Res.*, **19**, 559 (1963).

(80) H. J. Maria and S. P. McGlynn, *J. Mol. Spectrosc.*, **42**, 296 (1972).

(81) H. J. Maria and S. P. McGlynn, *J. Chem. Phys.*, **52**, 3399 (1970).

(82) L. W. Johnson, H. J. Maria, and S. P. McGlynn, *J. Chem. Phys.*, **54**, 3823 (1971).

(83) H. Basch, M. B. Robin, and N. A. Kuebler, *J. Chem. Phys.*, **49**, 5007 (1968).

(84) S. P. Peyerimhoff and R. J. Buenker, *J. Chem. Phys.*, **50**, 1846 (1969); S. P. Peyerimhoff, *ibid.*, **47**, 349 (1967).

(85) S. P. McGlynn, P. Hochmann, and H. J. Maria, "Excited States of Matter", C. W. Shoppee, Ed., Texas Tech University Press, Lubbock, 1973.

(86) R. F. Chen, *Luminescence News*, **9**, 9 (1975).

(87) R. O. Rahn and L. C. Landry, *Photochem. Photobiol.*, **18**, 29 (1973).

(88) R. O. Rahn, "Excited States in Organic Chemistry and Biochemistry", B. Pullman and N. Goldman, Eds., D. Reidel, Dordrecht, 1977; pp 27–37.

(89) R. O. Rahn, M. D. C. Battista, and L. C. Landry, *Proc. Natl. Acad. Sci. U.S.A.* in press.